Application of three sound scattering models to threadfin shad (*Dorosoma petenense*)

Josef M. Jech[a)]
North Carolina State University, Zoology Department, Box 7617, Raleigh, North Carolina 27695

D. M. Schael
Aquatic Ecology Laboratory, 227 Research Center, 1314 Kinnear Road, Columbus, Ohio 43212

C. S. Clay
Geophysical and Polar Research Center, University of Wisconsin, Madison, Wisconsin 53706

(Received 18 December 1993; revised 16 February 1995; accepted 11 May 1995)

Three sound scattering models [T. K. Stanton, J. Acoust. Soc. Am. **86**, 691–705 (1989), C. S. Clay, J. Acoust. Soc. Am. **89**, 2168–2179 (1991), and C. S. Clay and J. Horne, J. Acoust. Soc. Am. **96**, 1661–1668 (1994)] were used to model backscatter measurements from individual threadfin shad. Thirty three threadfin shad from Lake Norman, North Carolina were insonified at 120, 200, and 420 kHz to determine acoustic backscattering cross sections. The measurements covered the range of fish total length (TL) over acoustic wavelength (λ) of $4<\mathrm{TL}/\lambda<25$. The finite bent cylinder and low-resolution acoustic scattering models require conversion of fish body and swimbladder morphology to equivalent cylindrical parameters. There appears to be a direct relationship between fish morphology and cylindrical parameters. The ray-mode model uses the actual morphology of the swimbladder and body. Probability density functions (PDF's) from the same fish at 120 and 420 kHz support the idea that knowledge of fish orientation in the field is important and the effect of orientation becomes more significant at higher frequencies. The scattering curves can be used in the inverse method along with multiple frequency sonar systems to investigate the adequacy of classification and identification of fish. © *1995 Acoustical Society of America.*

PACS numbers: 43.30.Ft, 43.30.Gv, 43.30.Sf

LIST OF SYMBOLS

ρ	density of medium (kg/m^3)
c	speed of sound in medium (m/s)
λ	wavelength of sonar frequency in medium (m); $\lambda=c/f$
f	sonar (carrier) frequency (Hz)
k	wave number; $k=2\pi f/c$
γ	angle from perpendicular axis through the center of the cylinder
$\gamma_{\max}$	maximum value of γ, where $2\gamma_{\max}$ subtends the entire arc of the cylinder
r_c	radius of curvature for the cylinder
L	total length of the cylinder (m): for uniform bent cylinder model, L_{arc} is the total arc length; $L_{\mathrm{arc}}=2\gamma_{\max}r_c$ for low-resolution model; L=total length of the cylinder projected on the x axis
$\mathscr{S}$	scattering length or amplitude
L_0	unit reference scattering length; $L_0=1$ m
χ	$=r_c/L$. $\gamma_{\max}$, r_c, and χ describe cylinder deformation
a	radius of the cylinder (m)
α	cylinder deformation where $z(x)=\alpha x^2$ (m^{-1})
δ	empirical mode attenuation coefficient
TL	total length of the fish, measured from tip of snout to end of caudal fin (m)
M	modal series term, where $M+1$ is the total number of modal terms
J_m	cylindrical Bessel function of the first kind of order m
N_m	cylindrical Bessel function of the second kind of order m
J'_m	derivative of J_m
N'_m	derivative of N_m
N_e	number of volume elements for the ray-mode model
ϕ	azimuthal angle of receiver relative to source; $\phi=\pi$ for backscatter
ϵ_m	Neumann's number; $\epsilon_0=1$ and $\epsilon_{m>0}=2$
σ_{bs}	backscattering cross section (m^2); $\sigma_{\mathrm{bs}}=\lvert\mathscr{S}\rvert^2$
TS	target strength, $\mathrm{TS}=10\log_{10}(\sigma_{\mathrm{bs}}/L_0)$
i	$\sqrt{-1}$

INTRODUCTION

Considerable work has been done on the backscattering characteristics of fish and the relationship of acoustic backscatter to actual fish length.[1,2] Fish are complicated scatterers by the nature of their shape (cylindrical or spheroid), deformation (curvature of the body and swimbladder), and composition (body muscle, bone and fat, and swimbladder). These anatomical attributes combined with behavioral characteristics complicate the calculation of fish size from acoustic data and consequently in obtaining population density estimates in aquatic environments.[3] Two avenues of investi-

[a)]Present address: Great Lakes Center, SUNY College at Buffalo, 1300 Elmwood Ave., Buffalo, NY 14222.

 0001-4966/95/98(4)/2262/8/$6.00

gation into the relationship of fish size to acoustic backscatter are empirical acoustic measurements and modeling. Both have provided much information and are inexorably linked.

The measurement of backscatter from fish appears simple. One measures the backscatter amplitude from a number of various lengthed fish and computes a regression equation to calculate fish length from acoustic backscatter.[4] This method has been employed by fisheries acousticians for a number of years,[5] but has shortcomings when applied to specific species or communities.[6,7] Unfortunately, simple measurements reveal complicated variability. Fish orientation, behavior and variations in body and swimbladder shape affect backscatter measurements.[8–12] Probability density functions (PDF's) have been used to estimate activity levels of fish during backscattering measurements.[11] Measurements alone will not enable prediction of backscatter from fish populations. Modeling backscatter from fish is needed to explain measurement variability, improve the estimation of fish size and identify fish species from acoustic data.

Modeling the backscattering function for complicated shapes, such as fish, at high frequencies is difficult. The swimbladder is the dominant scattering organ in fish at typical fisheries survey frequencies (>30 kHz).[13,14] A fish swimbladder has a complex and dynamic shape. Therefore, attempts to model backscatter have transformed the fish body and swimbladder to simple shapes.[15–17] These transformations have met with limited success.[1] An important step was made by Foote,[18] who formed an acoustic model using the Kirchhoff approximation and morphology of the swimbladder. Recently, Stanton[19] described scattering from a finite bent cylinder, which approximates the shapes of zooplankton and fish. Clay[20] modified the finite bent cylinder model and applied it to anchovy measurements. Clay[21] also derived a ray-mode model from the Kirchoff approximation and a low mode solution. Clay and Horne[22] applied the ray-mode model, using actual morphology, to cod. These recent models are improvements in the modeling of backscatter because they allow more realistic approximations of fish body and swimbladder morphology.

In this paper, three scattering models, Stanton's finite bent cylinder model,[19] Clay's low-resolution acoustic scattering model[20] and Clay and Horne's ray-mode model[22] are used to construct backscatter curves for threadfin shad (*Dorosoma petenense*). Model results are compared to measurements of backscatter from individual threadfin shad. The PDF's of backscatter measurements of the same fish insonified at 120 and 420 kHz are compared to investigate effects of sonar frequency on the calculation of target strength. Application of these models will hopefully lead to better estimates of fish size and densities and the possibility of species identification in the field.

I. BACKSCATTER MODELS

Three scattering models are applied to acoustic data from individual threadfin shad. The equations used in this paper are given. For a more detailed derivation of each model, see Refs. 19–24. The generic term "cylinder" is used to denote either the fish body or the swimbladder, depending on which is being modeled. $\mathscr{S}$ is the scattering length or amplitude (denoted as $\not\sim$ in Ref. 19 and S in Ref. 20). Also note that the equations are for backscatter only ($\Theta=\pi/2$; $\sin\Delta/\Delta=1$, where $\Delta=kL\cos\Theta$).

A. Finite bent cylinder

The finite bent cylinder model computes $\mathscr{S}(f)$ for a finite uniformly bent cylinder

$$\mathscr{S}(f)=\frac{L_{\text{arc}}}{\pi\gamma_{\max}}\int_0^{\gamma_{\max}}\sum_{m=0}^{M} b_m \times\cos(m\phi)e^{2ikr_c(1-\cos\gamma)}d\gamma, \tag{1}$$

where $\phi=\pi$ for backscatter. Here b_m is

$$b_m=\frac{-\epsilon_m}{1+iC_m} \tag{2}$$

and C_m is

$$C_m=\frac{J_m'(k_1a)N_m(ka)-ghN_m'(ka)J_m(k_1a)}{J_m'(k_1a)J_m(ka)-ghJ_m'(ka)J_m(k_1a)},$$

$$g=\rho_1/\rho_w,\quad h=c_1/c_w, \tag{3}$$

where the subscripts "1" and "w" denote wave number, density and sound speed, in the cylinder and surrounding water, respectively. The fish body and swimbladder are converted to a finite uniformly bent cylinder of total arc length, L_{arc}, where $\gamma_{\max}$, r_c, and χ describe cylinder deformation (Fig. 1).

B. Low-resolution acoustic model

The low-resolution acoustic model modifies Eq. (1) by moving the summation of b_m and $\cos(m\phi)$ out of the integral and inserting a roughness attenuation (A_m)

$$\mathscr{S}(f)=\frac{-i}{\pi}\sum_{m=0}^{M} b_m\cos(m\phi)A_m\int_0^{L}e^{i2kz(x)}\,dx, \tag{4}$$

where A_m is

$$A_m=e^{-\delta k^2a^2}, \tag{5}$$

x denotes the along-cylinder axis, $z(x)$ denotes the perpendicular distance the cylinder is deformed, and L is the length of the cylinder as projected to the x axis (Fig. 1). The phase shift $i2kr_c(1-\cos\gamma)$ is simplified to a parabolic function, $z(x)=\alpha x^2$. The phase shift integral can be evaluated using a change of variables and computing Fresnel integrals. So that

$$A_z=\int_0^{L}e^{i2kz(x)}dx=\sqrt{\frac{\pi}{4k\alpha}}\,[C_F(\zeta)+iS_F(\zeta)], \tag{6}$$

where C_F and S_F are the Fresnel integrals

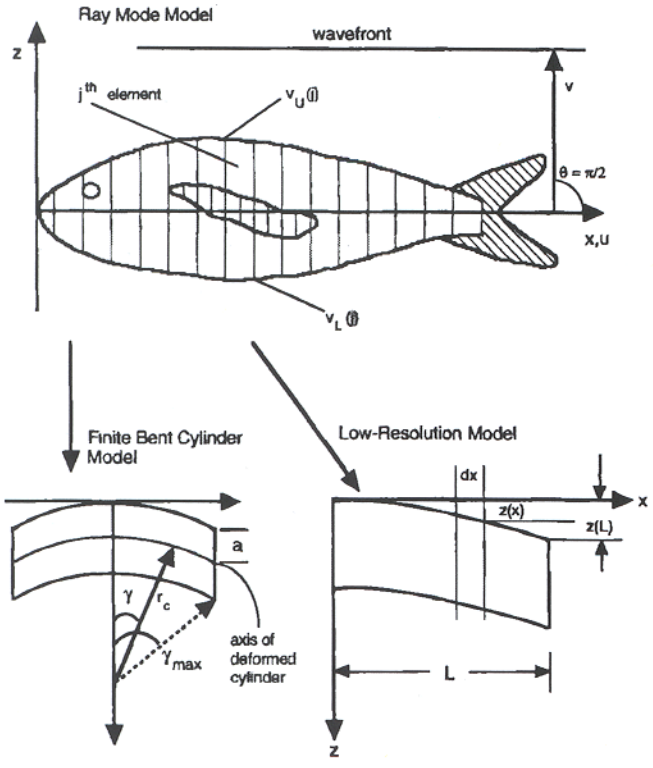

FIG. 1. General diagrams of the conversion from threadfin shad morphology to equivalent cylindrical shape. The fish body and swimbladder were treated individually. The upper sketch is the threadfin shad used for the ray-mode model with swimbladder. The incident plane wave arrives from above the fish (dorsal aspect) and bent cylinder ($\Theta=\pi/2$). Thus the coordinate systems x, z and U, V are equal for the ray-mode model. Fish body and swimbladder are sectioned into cylinders (jth element). The lower sketches show the geometry of the uniformly bent cylinder for the finite bent cylinder model (left) and the low-resolution model (right).

$$C_F(\zeta)=\int_0^{\zeta}\cos\left(\frac{\pi}{2}\xi^2\right)d\xi, \tag{7}$$

$$S_F(\zeta)=\int_0^{\zeta}\sin\left(\frac{\pi}{2}\xi^2\right)d\xi, \tag{8}$$

$$\zeta=\sqrt{4ka/\pi}\,L, \tag{9}$$

(see Abramowitz and Stegun[25] for details on integrating). Now Eq. (4) can be written as

$$\mathscr{B}(f)=\frac{-i}{\pi}\sum_{m=0}^{M} b_m\cos(m\phi)A_mA_z. \tag{10}$$

Similar to the finite bent cylinder model, the fish swimbladder and body are converted to a uniformly bent cylinder where cylinder length, L, is the length of the cylinder projected onto the x axis (Fig. 1).

C. Ray-mode model

The Ray-mode model describes scattering from fish using a low-mode cylinder solution, a Kirchhoff ray approximation and morphology of the fish. The morphology of the fish body and swimbladder, obtained by dissection or x rays, is used to construct the volume elements (Fig. 1). The fish can be rotated and transferred from x-z coordinates to a u-v coordinate system as in Ref. 22. In all following equations, the wavefront is in dorsal aspect ($\Theta=\pi/2$). Backscatter from each individual element is computed as a finite cylinder, and these are summed over the whole swimbladder or body. For the swimbladder only and $ka<0.2$, a low mode ($M=0$) cylinder solution is used. Equation (4) is modified, where the roughness coefficient, A_m, is eliminated and the phase shift $e^{i2kz(x)}$ is replaced with the geometry of the swimbladder ($v(x)$). For mode $M=0$, Eq. (4) can be written as the sum of the scatter for N_e elements

$$\mathscr{B}(f)=\frac{-i}{\pi}\sum_{j}^{N_e} b_0e^{-i2kv(j)}\,dx(j). \tag{11}$$

For the swimbladder and $ka>0.2$, a Kirchhoff ray approximation is used. Equation (11) in Ref. 21 is modified to sum the backscatter from N_e swimbladder elements

$$\mathscr{B}(f)=-i\frac{\mathscr{R}_{fs}(1-\mathscr{R}^2_{wf})}{2\sqrt{\pi}}\sum_{j=0}^{N_e-1}A_{sb}(k_{fb}a(j)+1)^{1/2}\times e^{-i(2k_{fb}v_U(j)+\Psi_{sb})}\Delta u(j),$$

$$A_{sb}=\frac{ka(j)}{ka(j)+0.083},\quad \Psi_{sb}=\frac{ka(j)}{(40+ka(j))}-1.05,$$

$$\mathscr{R}_{fs}=\frac{g'h'-1}{g'h'+1},\quad \mathscr{R}_{wf}=\frac{\rho_{fb}c_{fb}-\rho_wc_w}{\rho_{fb}c_{fb}+\rho_wc_w},$$

$$g'=\frac{\rho_{sb}}{\rho_{fb}},\quad h'=\frac{c_{sb}}{c_{fb}}, \tag{12}$$

A similar expression is derived for the fish body

$$\mathscr{B}(f)=-i\frac{\mathscr{B}_{wf}}{2\sqrt{\pi}}\sum_{j=0}^{N_e-1}(ka(j))^{1/2}[e^{-i2kv_U(j)}-(1-\mathscr{R}^2_{wf})e^{i(-2kv_U(j)+2k_{fb}(v_U(j)-v_L(j))+\Psi_{fb})}]\times\Delta u(j), \tag{13}$$

$$\Psi_{fb}=-\frac{\pi k_{fb}v_U(j)}{2(k_{fb}v_U(j)+0.4)},\quad k_{fb}=\frac{2\pi f}{c_{fb}},$$

where $\mathscr{R}$ is the reflection coefficient, subscript "wf" denotes the water–fish body interface, "fs" denotes the swimbladder–fish body interface, "fb" refers to the fish body, "sb" refers to the swimbladder, and U and L refer to the upper and lower surfaces in u-v coordinates, respectively. Here, $\Delta u(j)$ denotes incremental distance between elements and A_{sb} and Ψ are empirical amplitude and phase adjustments for small ka.

The backscattering cross section (σ_{bs}) can be computed from the complex $\mathscr{B}(f)$ for all three models by

$$\sigma_{bs}(f)=|\mathscr{B}(f)|^2. \tag{14}$$

Reduced σ_{bs} is

$$\text{reduced }\sigma_{bs}(f)=|\mathscr{B}(f)|^2/\text{TL}^2 \tag{15}$$

and the reduced target strength (TS) is

$$\text{reduced TS}=20\log_{10}[|\mathscr{B}(f)|/\text{TL}]. \tag{16}$$

TABLE I. Model parameters.

Water	C	1460 m/s
	ρ	1000 kg/m^3
Fish body	C_1	1570 m/s
	ρ_1	1080 kg/m^3
	L	0.0746 m
	a	0.0023 m
	α	9.794 m^{-1}
	δ	0.03
	χ	0.2 (0.25)
Swimbladder	C_1	340 m/s
	ρ_1	2.64 kg/m^3
	L	0.0224 m
	a	0.0015 (0.0017) m
	α	12 m^{-1}
	δ	0.01
	χ	0.5 (0.75)
	M	2

The scattering lengths for the fish body and swimbladder were computed individually. Whole fish scatter ($\mathscr{L}_{wf}(f)$) can be computed from the fish body ($\mathscr{L}_{fb}(f)$) and swimbladder ($\mathscr{L}_{sb}(f)$). Coherent scatter is assumed and thus $\mathscr{L}_{fb}(f)$ and $\mathscr{L}_{sb}(f)$ add as the complex functions

$$\mathscr{L}_{wf}(f)=\mathscr{L}_{fb}(f)+\mathscr{L}_{sb}(f). \tag{17}$$

Values for equivalent cylindrical parameters and physical variables used in the backscatter models are given in Table I. Water c and ρ were computed for freshwater. Fish body c and ρ were approximated from Ref. 20. Swimbladder c and ρ were computed for a swimbladder at 10 m depth. Here, $M=2$ was used for both swimbladder and body in the finite bent cylinder and low-resolution models, where, $M+1$ is the number of modal series terms (0 to M). A constant mode attenuation (δ), estimated from Ref. 20, is used for the swimbladder and body individually.

II. ACOUSTIC AND MORPHOLOGY MEASUREMENTS

Acoustic data were taken in Lake Norman, a reservoir in western North Carolina. Backscatter data from 33 live threadfin shad were obtained by individually tethering each fish with monofilament fishing line through the upper and lower maxilla. A 3-lb triangular weight was attached to the end of the line, 1 m below the fish to keep the fish in a dorsal aspect relative to the transducer. The fish were lowered to a depth of approximately 10 m directly under the transducer. Most of the data were collected with individual fish on a line, but in some cases 3–5 fish were placed on a line at 1-m intervals for data collection (Table II). Target strength data were collected with a Biosonics dual-beam acoustic system at the three frequencies, 120, 200, and 420 kHz. Beam widths (defined by the total angular width between half power points of the one-way diffraction pattern) of the narrow/wide beams were 120 kHz-10°/25°, 200 kHz-6°/15°, and 420 kHz-6°/15°. Not all fish were insonified at all three frequencies (Table II). Fish used for empirical measurement of target strength ranged from 53–111 mm TL ($\sim 4<TL/\lambda<\sim 23$), and the number of pings (N) used to calculate the mean backscatter (σ_{bs}) of each fish ranged from 10 to 1200 (Table II). Mean target strength ($\overline{TS}$) was computed by $10*\log(\sigma_{bs})$. Reduced backscatter and TS were computed from Eqs. (15) and (16). The Biosonics system gives the off-axis (in dB) position of the fish for each ping. Data chosen for analysis were on or near the transducer axis, i.e., the "dB position" was between 0 and −2 dB. The 2-dB ring corresponds to 7.7°, 3.9°, and 5.2° off the transducer axis for the 120-, 200-, and 420-kHz sonars, respectively.

The finite bent cylinder and low-resolution models require conversion from fish morphology to equivalent cylindrical parameters (length, radius, and curvature). Morphological measurements of the swimbladder and fish body were taken on ten threadfin shad preserved in ethanol obtained at a later date (not the same individuals used in the backscattering experiments). Individual fish were measured (TL, body depth, and width) and then dissected to obtain measurements of the swimbladder (length along the axis of the swimbladder, width, and depth) (Table III). Linear regressions of these measurements were used to define the relationships of fish body TL to body depth and width and swimbladder width, depth and length (Table III). These regressions were used to compute equivalent cylindrical parameters. The mean TL (computed from the shad TL's used in the backscatter measurements, Table II) was used to compute an average fish body length. The fish body was then converted to a cylinder of equal volume. The swimbladder was assumed to be cylindrical in shape. The cylindrical parameters were then varied to (1) fit the $\mathscr{L}(f)$ curves to the data and (2) investigate sensitivity of the models to the cylindrical parameters of radius (a) and curvature (χ) (Table I).

Fish body and swimbladder morphology for the ray-mode model were obtained by dissecting a single threadfin shad, while maintaining the integrity of the swimbladder, and photocopying the dissected fish. The photocopy was digitized and used to section the body and swimbladder into N_e cylindrical elements (Fig. 1). The morphology regression equations (Table III) were used to compute the body and swimbladder radius for each element.

III. COMPARISON OF ACOUSTIC MODELS AND ACOUSTIC MEASUREMENTS

The finite bent cylinder and low-resolution acoustic scattering models (ASM's) are more sensitive to variations in swimbladder morphology than body morphology. The low-resolution model shows that the fish body has lower overall backscatter [Fig. 2(a)] than does the swimbladder [Fig. 2(b)], but does become more important at $TL/\lambda>20$. Scattering length functions for the fish body and swimbladder were added coherently as the sum of the complex functions [Eq. (12)] to give the whole fish backscatter function [Fig. 2(c)]. Data points in Figs. 2–4 are reduced backscatter values from individual acoustic measurements (Table II). The scattering length curve is sensitive to swimbladder radius (a) and curvature (χ). In the finite bent cylinder model L_{arc} was held constant for both the swimbladder and fish body and increasing χ corresponds to straighter cylinders. The reduced scattering length for body $\chi=1.0$, swimbladder $a=0.015$ m and swimbladder $\chi=0.5$, will be used as a reference [Fig. 3(a)].

TABLE II. Backscatter measurements from individual threadfin shad.

Sonar frequency (kHz)	Fish TL (mm)	N	TL/λ	$\overline{\sigma_{bs}}$ (m^2)	$\overline{TS}$ (dB)	$\frac{\lvert\mathcal{S}\rvert}{TL}$	$20\log\left[\frac{\lvert\mathcal{S}\rvert}{TL}\right]$
120	+61	294	5.01	2.75e-06	−55.6	0.027	−31.3
120	+61	52	5.01	2.50e-06	−56.0	0.026	−31.7
120	+55	109	4.52	2.22e-06	−56.5	0.027	−31.3
120	+62	29	5.10	2.41e-06	−56.2	0.025	−32.0
120	+62	168	5.10	1.38e-05	−48.6	0.060	−24.4
120	++54	286	4.44	3.97e-06	−54.0	0.037	−28.7
120	++56	233	4.60	3.68e-06	−54.4	0.034	−29.3
120	++57	106	4.68	3.07e-06	−55.1	0.031	−30.2
120	++57	109	4.68	9.39e-06	−50.3	0.054	−25.4
120	++53	130	4.36	7.32e-06	−51.4	0.051	−25.8
120	+++106	48	8.71	4.36e-06	−53.6	0.020	−34.1
120	+++105	31	8.63	4.04e-06	−53.9	0.019	−34.3
120	+++111	795	9.12	7.87e-06	−51.0	0.025	−31.9
120	94	11	7.73	3.79e-06	−54.2	0.021	−33.7
120	*61	214	5.01	4.51e-06	−53.5	0.035	−29.2
120	**62	118	5.10	3.76e-06	−54.3	0.031	−30.1
120	***66	668	5.42	3.59e-06	−54.5	0.029	−30.8
120	****58	10	4.77	2.67e-06	−55.7	0.028	−31.0
200	70	661	9.59	4.85e-06	−53.1	0.032	−30.0
200	82	130	11.23	2.61e-06	−55.8	0.020	−34.1
200	76	197	10.41	1.00e-05	−49.9	0.042	−27.6
200	86	587	11.78	3.15e-06	−55.0	0.021	−33.7
200	78	125	10.68	5.37e-06	−52.7	0.030	−30.5
200	85	94	11.64	3.58e-06	−54.5	0.022	−33.0
200	95	248	13.01	1.70e-06	−57.7	0.014	−37.3
200	91	60	12.47	7.56e-06	−51.2	0.030	−30.4
200	96	97	13.15	8.17e-06	−50.9	0.030	−30.5
420	70	173	20.14	8.33e-06	−50.8	0.041	−27.7
420	*61	600	17.55	5.70e-06	−52.4	0.039	−28.2
420	**62	584	17.84	6.41e-06	−51.9	0.041	−27.8
420	***66	435	18.99	7.83e-06	−51.1	0.042	−27.5
420	****58	1200	16.68	6.97e-06	−51.6	0.046	−26.4
420	70	311	20.14	5.60e-06	−52.5	0.034	−29.4

Sonar frequency λ (m)		
	120 kHz	0.0122
	200 kHz	0.0073
	420 kHz	0.00348

* denotes same fish insonified by the 120- and 420-kHz sonar frequency.

\+ denotes multiple fish on the same line when insonified.

Increasing the swimbladder radius 2 mm (a=0.017 m) and straightening the swimbladder (χ=0.75) results in a scattering curve with less maxima and minima [Fig. 3(b)]. Increasing χ to 1.0 follows a similar trend, with an increase in the overall scattering amplitude [Fig. 3(c)]. A straighter body cylinder (χ=5.0) has little effect on whole fish scatter at lower frequencies, however scatter from the fish body does become important above TL/λ>20 [compare Fig. 3(d) to (b)].

The ray-mode model can be described as a "fish model" because the scattering length curve is computed from the actual morphology of the fish swimbladder and body. Conversion to a cylindrical shape is not required and as such, the ray-mode model can be viewed as more realistic than the finite bent cylinder or low-resolution models. Figure 4(a) presents the ray-mode scattering curve in linear units. Fisheries acoustics data is often presented in terms of target strength, and Fig. 4(b) shows the ray-mode scattering length curve for reduced TS.

IV. RELATIONSHIP OF FISH MORPHOLOGY TO CYLINDRICAL PARAMETERS

Agreement of the finite bent cylinder and low-resolution models with data suggest a simple relationship between morphometric relationships and equivalent cylindrical parameters, although slight adjustments are needed. The body shape of the threadfin shad is a laterally flattened ellipsoid, and conversion to an equivalent cylindrical shape is required. For the fish body, TL was used as the equivalent cylindrical length (L) and the regressions for depth and width were used in the calculation of equivalent cylindrical radius (a) (Table III). Deformation of the equivalent body cylinder required more curvature than measured from the fish body. Fish body

TABLE III. Threadfin shad fish morphology measurements and equations used to convert the fish body and swimbladder to equivalent cylindrical parameters.

TL (mm)	Body depth (mm)	Body width (mm)	Swimbladder length (mm)	Swimbladder width (mm)	Swimbladder depth (mm)
70	19.5	6.0	19.5	3.0	5.4
53	13.4	4.2	14.7	1.5	3.2
60	16.8	5.3	11.0	2.8	3.7
60	17.4	5.0	15.0	2.5	3.5
105	29.6	9.0	27.0	3.3	6.3
93	25.5	8.4	25.0	3.5	6.6
84	24.3	6.9	24.0	2.9	4.1
66	17.9	5.3	16.7	3.5	3.3
63	17.0	4.9	11.9	3.0	4.9
58	14.2	4.0	11.9	2.7	3.2

Equations for equivalent cylindrical parameters.

Fish body	Fish swimbladder
L=total length (TL)	L=0.3*TL
depth=0.275*TL	depth=0.0621*TL
width=0.083*TL	width=0.0394*TL
$a=\sqrt{\frac{\text{depth*width}}{24}}$	$a=\frac{\text{width}}{2}$

α=9.794 m^{-1} corresponds to a more curved body than does approximating $z(L)$ as depth/2 (α=7.4 m^{-1}).

Swimbladder shape is nearly cylindrical and conversion to a cylinder requires only measurements of the swimbladder. Swimbladder radius was converted directly from width/2. The equivalent cylindrical length was longer than the measured length. The regression resulted in a swimbladder approximately 0.25*TL, whereas 0.3*TL was needed to calculate swimbladder L (Table III). Swimbladder length was measured as the linear distance from anterior to posterior ends. The authors would like to note that a single measured length (i.e., $L=L_{arc}$) was used in each respective model and that each model uses this length differently. This was done to see if simple morphological measurements can be implemented into the models. While some adjustments were needed, agreement of the data to models suggest morphological measurements of the swimbladder and body can be used in the models. For the low-resolution model, $\alpha\cong 9$ corresponds to 12° below horizontal. α=12 gave the best fit to the data, which corresponds to the swimbladder about 15° below the horizontal axis. Whitehead and Blaxter[26] show a threadfin shad swimbladder 12° below horizontal. Due to the problems associated with preservation and dissection, morphology of the swimbladder is tedious to obtain. X rays of live fish may solve problems associated with swimbladder measurements.

A. PDF's

The probability density functions (PDF's) of echo amplitudes for the three fish insonified at both 120 and 420 kHz were compared to investigate frequency effects on backscatter from fish. The PDF's for the 66-mm fish (Table II, denoted with ***) insonified at 120 [Fig. 5(a)] and 420 kHz [Fig. 5(b)] are given as representative examples. A Rician PDF was fit to the fish echo PDF's. $\gamma(\gamma$ is different than used

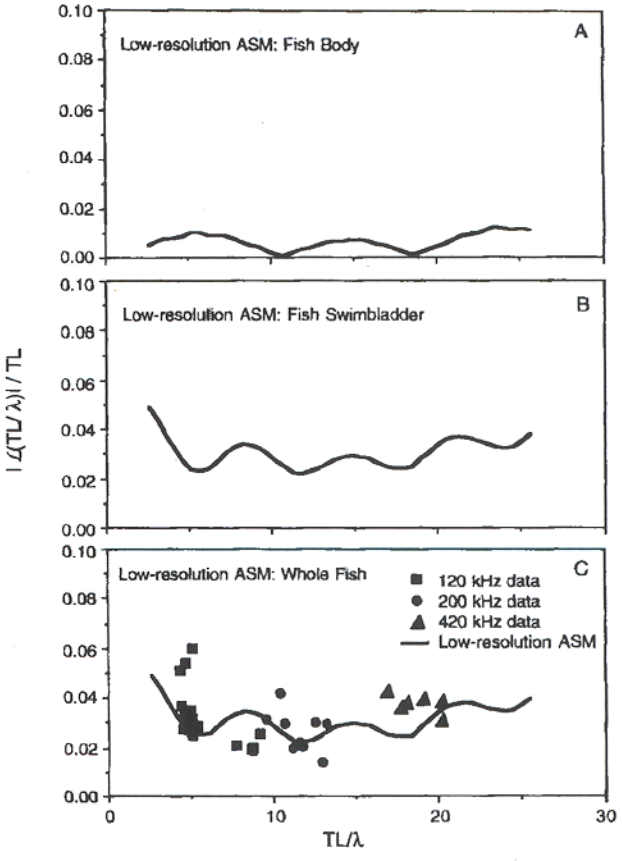

FIG. 2. (a) Reduced scattering length curve computed by the low-resolution acoustic scattering model (ASM) for the fish body. (b) Reduced scattering length curve for the fish swimbladder. (c) Reduced scattering length curve computed by summing the complex functions from the fish body and swimbladder (whole fish backscatter). Data points are reduced backscatter measurements of individual threadfin shad at the three frequencies: 120 (squares), 200 (circles), and 420 kHz (triangles).

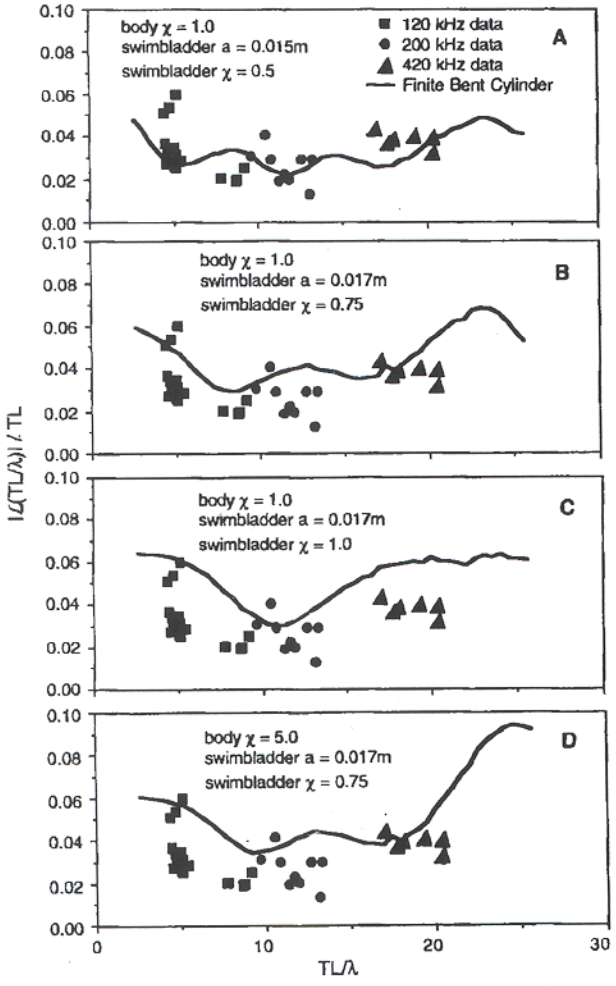

FIG. 3. Whole fish reduced scattering length curve computed from the finite bent cylinder model where (a) body χ=1.0, swimbladder a=0.015 m, and swimbladder χ=0.5; (b) body χ=1.0, swimbladder a=0.017 m, and swimbladder χ=0.75; (c) body χ=1.0, swimbladder a=0.017 m, and swimbladder χ=1.0 (d) body χ=5.0, swimbladder a=0.017 m. and swimbladder χ=0.75. Data points are the same as Fig. 2.

in the acoustic models) is a measure of the variability in echo amplitudes, where higher values indicate lower variability and γ=1 indicates a Rayleigh distribution.[11] At 120 kHz, a γ of 10 fit the unimodal PDF and at 420 kHz, a γ of 3.8 fit the bimodal PDF [Fig. 5(a) and (b), respectively]. The quantitative reasons for the change in γ and fish echo PDF are unknown to the authors. Orientation of the insonified fish relative to the sonar transducer is known to affect the backscatter PDF.[8–12] Nakken and Olsen[8] show that at higher sonar frequencies, small changes in orientation (from dorsal aspect) have greater effects on backscattering amplitude than at lower frequencies. The threadfin shad were tethered at the head, allowing small changes in horizontal orientation. Assuming similar behavior between the 120- and 420-kHz measurement periods, small changes in horizontal orientation may cause the observed differences in the PDF's between the two frequencies.

V. CONCLUSIONS

Three acoustic scattering models were used to calculate scattering length curves for threadfin shad. The curves were

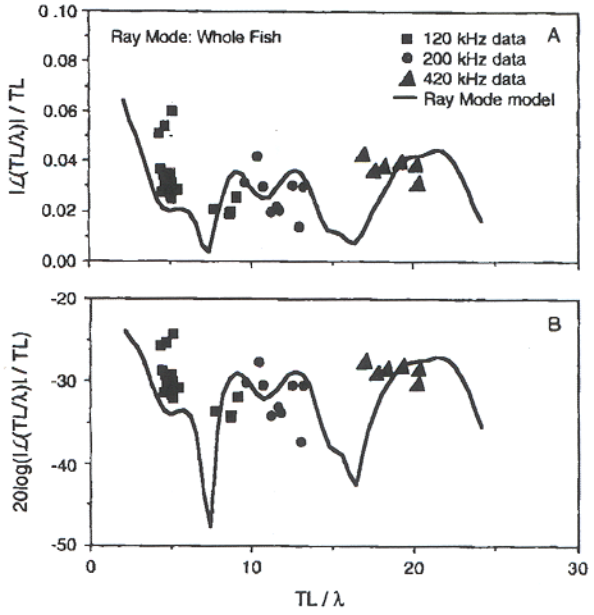

FIG. 4. (a) Reduced scattering length curve computed by the ray-mode model in linear units. (b) Reduced scattering length in logarithmic form. Curves are computed from fish morphology. Data points are same as Fig. 3.

compared to acoustic backscatter measurements from individual threadfin shad in Lake Norman, North Carolina. The finite bent cylinder model and the low-resolution acoustic

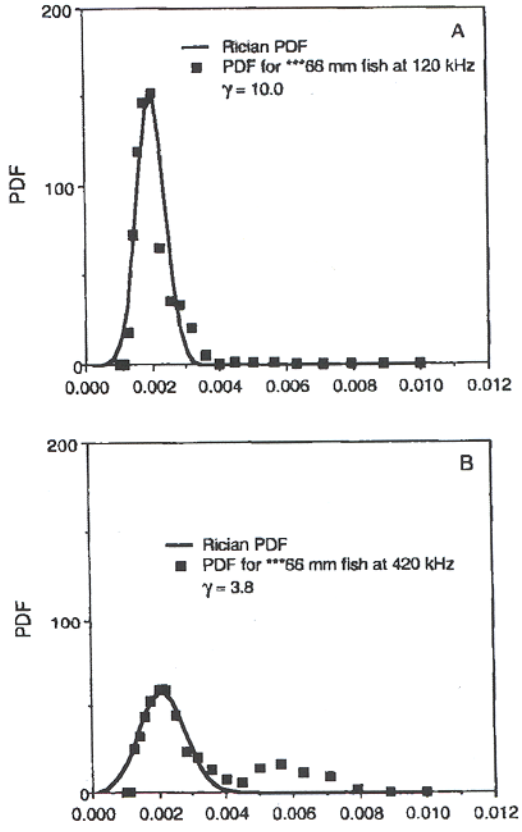

FIG. 5. PDF's for the 66-mm fish (denoted by *** in Table II) insonified at (a) 120 and (b) 420 kHz. Solid square symbols are echo amplitude PDF's from target strength data and the solid line is the Rician PDF.

models require conversion of fish morphology to equivalent cylindrical parameters. Conversion equations suggest that morphological characteristics of the fish body and swimbladder can be measured and converted to equivalent cylindrical parameters. The finite bent cylinder model and the low-resolution models are more sensitive to swimbladder radius and curvature and less sensitive to body parameters. The ray-mode model uses actual fish morphology and is a more realistic fish model.

Morphometric parameters from a few fish, in the finite bent cylinder and low-resolution models, and only a single fish, for the ray-mode model, were used to compute scattering curves which corresponded to backscatter measurements from several fish. This suggests that only a few fish are needed to model scattering for a species population at a particular life stage. This may be important because it reduces the amount of time and effort to construct scattering curves for fish. The scattering curves may be useful for size class estimates or discriminating and identifying fish types or species. PDF's of echo amplitude for the same fish insonified at 120 and 420 kHz show different distributions, suggesting complex scattering behavior for multiple frequencies.

The scattering curves for fish can be used in the inverse problem to obtain size class information of fish.[27] Multiple frequency systems have successfully given size-class information for zooplankton[28,29] and fish.[27] Zooplankton and fish have been modeled as fluid spheres, thus treating all organisms as generic "zooplankton" or "fish." It is now possible to better describe sound scattering from fish with the bent cylinder and ray-mode models. Holliday[30] extended the inverse method for one scattering type (i.e., fish with swimbladders) to two types (i.e., fish with swimbladders versus fish without swimbladders). Given the possibility to define a specific backscatter curve for each particular species or type of fish, the inverse method computes the length-frequency distributions for each fish species or type. Refinement of the scattering models for different fish body and swimbladder forms may ultimately lead to acoustic identification of fish species.

ACKNOWLEDGMENTS

Funding for J. M. Jech was provided by the South Atlantic Bight Recruitment Experiment (SABRE), NOAA Coastal Ocean Program #NA16RGO492-01 with additional support from NSF #DCE-9415740 to S. Brandt. Funding for D. M. Schael was provided by Duke Power Company. The authors would like to thank Don Degan for useful comments and Duke Power personnel for assistance in acoustic data collection and purse seine data. Randy Jackson provided the threadfin shad for morphological measurements.

[1] L. Midttun, "Fish and other organisms as acoustic targets," Rapp. P.-V. Réun. Cons. Int. Explor. Mer. **184**, 25–33 (1984).

[2] K. G. Foote, "Summary of methods for determining fish target strength at ultrasonic frequencies," J. Cons. Int. Explor. Mer. **48**(2), 211–217 (1991).

[3] A. D. Hawkins, "Some biological sources of error in the acoustical assessment of fish abundance," in *Meeting on Hydroacoustical Methods for the Estimation of Marine Fish Populations*, Cambridge, MA, June 1979 (Draper Lab., Cambridge, MA, 1981).

[4] R. H. Love, "Measurements of fish target strength: A review," Fish. Bull. **69**, 703–715 (1971).

[5] D. N. MacLennan and E. J. Simmonds, *Fisheries Acoustics* (Chapman and Hall, London, 1992).

[6] K. G. Foote, "Analysis of some errors associated with the use of target strength-to-length regressions in estimating fish abundance," in *Meeting on Hydroacoustical Methods for the Estimation of Marine Fish Populations*, Cambridge, MA, June 1979 (Draper Lab., Cambridge, MA, 1981).

[7] K. G. Foote, "Systematic species and frequency dependent differences among gadoid target strength functions," in *Meeting on Hydroacoustical Methods for the Estimation of Marine Fish Populations*, Cambridge, MA, June, 1979 (Draper Lab., Cambridge, MA, 1981).

[8] O. Nakken and K. Olsen, "Target strength measurements of fish," Rapp. P.-V. Réun. Cons. Int. Explor. Mer. **170**, 52–69 (1977).

[9] K. Huang and C. S. Clay, "Backscattering cross-sections of live fish: PDF and aspect," J. Acoust. Soc. Am. **67**, 795–802 (1980).

[10] J. E. Ehrenberg, T. J. Carlson, J. J. Carlson, and N. J. Williamson, "Indirect measurement of the mean acoustic backscattering cross-section of fish," J. Acoust. Soc. Am. **69**, 955–962 (1981).

[11] C. S. Clay and B. G. Heist, "Acoustic scattering by fish-acoustic models and a 2-parameter fit," J. Acoust. Soc. Am. **75**, 1077–1083 (1984).

[12] G. C. Goddard and V. G. Welsby, "The acoustic target strength of fish," J. Cons. Int. Explor. Mer. **42**, 197–211 (1986).

[13] R. W. G. Haslett, "Measurement of the dimensions of fish to facilitate calculations of echo-strength in acoustic fish detection," J. Cons. Int. Explor. Mer. **27**, 261–269 (1962).

[14] R. W. G. Haslett, "The target strengths of fish," J. Sound Vib. **9**, 181–191 (1969).

[15] F. R. Harden Jones and G. Pearce, "Acoustic reflection experiments with perch (*Perca fluviatilis*) Linn. to determine the proportion of the echo returned by the swimbladder," J. Exp. Biol. **35**, 437–450 (1957).

[16] R. W. G. Haslett, "Determination of the acoustic scatter patterns and cross sections of fish models and ellipsoids," Br. J. Appl. Phys. **13**, 611–620 (1962).

[17] R. A. Saenger, "Swimbladder size variability in mesopelagic fish and bioacoustic modeling," J. Acoust. Soc. Am. **84**, 1007–1017 (1988).

[18] K. G. Foote, "Rather-high-frequency sound scattering by swimbladdered fish," J. Acoust. Soc. Am. **78**, 688–700 (1985).

[19] T. K. Stanton, "Sound scattering by cylinders of finite length. III. Deformed cylinders," J. Acoust. Soc. Am. 86, 691–705 (1989).

[20] C. S. Clay, "Low-resolution acoustic scattering models: Fluid-filled cylinders and fish with swimbladders," J. Acoust. Soc. Am. **89**, 2168–2179 (1991).

[21] C. S. Clay, "Composite ray-mode approximations for backscattered sound from gas-filled cylinders and swimbladders," J. Acoust. Soc. Am. **92**, 2173–2180 (1992).

[22] C. S. Clay and J. K. Horne, "Acoustic models of fish: The Atlantic cod (*Gadus morhua*)," J. Acoust. Soc. Am. **96**, 1661–1668 (1994).

[23] T. K. Stanton, "Sound scattering by cylinders of finite length. I. Fluid cylinders," J. Acoust. Soc. Am. **83**, 55–63 (1988).

[24] T. K. Stanton, "Sound scattering by cylinders of finite length. II. Elastic cylinders," J. Acoust. Soc. Am. **83**, 64–67 (1988).

[25] M. Abramowitz and I. A. Stegun, *Handbook of Mathematical Functions with Formulas, Graphs and Mathematical Tables*, Washington, National Bureau of Standards (Dover, New York, 1972).

[26] P. J. P. Whitehead and J. H. Blaxter, "Swimbladder form in clupeoid fishes," Zool. J. Linnean Soc. **97**, 299–372 (1989).

[27] D. V. Holliday, "Use of acoustic frequency diversity for marine biological measurements," in *Advanced Concepts in Ocean Measurements for Marine Biology*, edited by F. P. Diemer *et al.* (B. W. Baruch Library in Marine Science #10, 1980), pp. 423–460.

[28] D. V. Holliday, R. E. Pieper, and G. S. Kleppel, "Determination of zooplankton size and distribution with multifrequency acoustic technique," J. Cons. Int. Explor. Mer. **46**, 52–61 (1989).

[29] R. E. Pieper, D. V. Holliday, and G. S. Kleppel, "Quantitative zooplankton distributions from multifrequency acoustics," J. Plankton Res. **12**(2), 433–441 (1990).

[30] D. V. Holliday, "Extracting bio-physical information from the acoustic signature of marine organisms," in *Oceanic Sound Scattering Prediction*, edited by N. R. Anderson and B. J. Zahuranec (Plenum, New York, 1977).